A SURVEY OF 12.2 GHz METHANOL MASERS AND THEIR POLARIZATION PROPERTIES

BON-CHUL KOO, DAVID R. W. WILLIAMS, CARL HEILES, AND DONALD C. BACKER
Astronomy Department and Radio Astronomy Laboratory, University of California, Berkeley
Received 1987 June 1; accepted 1987 September 4

ABSTRACT

Methanol emission at 12.1786 GHz ($2_0 \rightarrow 3_{-1}$ E) has been searched for toward 78 nonstellar H_2O masers and 33 type I OH/IR stars. Eleven new methanol sources were found in nonstellar water masers, whereas no sources were found in stellar masers. Most of the new sources show narrow lines with velocity widths smaller than 1 km s^{-1} and are probably masers. We present tentative evidence that the methanol masers are not all associated with H_2O and OH masers.

Polarization properties have also been observed for five strong sources including Cepheus A and G188.94+0.89, which were detected in this survey. Three sources, G188.94+0.89, Cepheus A, and NGC 7538, are completely unpolarized, 0% ± 3%, and the other two sources show a small amount of linear polarization: a few percent for W3(OH) and 10% ± 3% for NGC 6334.

Subject headings: interstellar: molecules — masers — polarization

I. INTRODUCTION

Since its maser emission in the $J_2 \rightarrow J_1$ E transitions was detected by Barrett, Schwartz, and Waters (1971) in Orion, interstellar methanol has been searched for toward numerous galactic sources in various transitions. Buxton *et al.* (1977) searched for the $J_2 \rightarrow J_1$ ($J = 2, 4, 6$) lines at 25 GHz toward 132 known H_2O, OH, and SiO masers, but detected no sources. Only recently has methanol maser emission been detected toward sources other than Orion. Wilson *et al.* (1984) discovered W3(OH) and probably NGC 7538 to be maser sources in the $9_2 \rightarrow 10_1$ A^+ emission, and Wilson *et al.* (1985) found W3(OH) to show maser emission in the $2_1 \rightarrow 3_0$ transition. Morimoto, Ohishi, and Kanzawa (1985) detected maser emission in the $4_{-1} \rightarrow 3_0$ E and $7_0 \rightarrow 6_1$ A lines toward Sgr B2, W51, and two other galactic sources. Also, Menten *et al.* (1986) observed the $J_2 \rightarrow J_1$ series towards 30 galactic sources and found maser emission in W31, W33, W51, and DR 21.

More recently, Batrla *et al.* (1987) detected yet another maser emission in the $2_0 \rightarrow 3_{-1}$ transition at 12.1786 GHz toward W3(OH), NGC 6334, NGC 7538, and several other galactic sources. The strength of this line in W3(OH) and NGC 6334F[1] was found to be of order 1000 Jy, which made them the strongest methanol masers ever found. We have searched for this newly discovered methanol emission in 78 nonstellar H_2O masers and 33 type I OH/IR stars. We found 11 new sources from nonstellar H_2O masers, but none from stellar masers.

We also performed polarization observations of this line in five strong sources. The polarization properties of methanol masers have not been observed, except for the $J_2 \rightarrow J_1$ emission in Orion by Hills, Pankonin, and Landecker (1975); they set an upper limit on the linear polarization of 20%. We found that two sources are weakly linearly polarized and the other three sources are not polarized.

II. OBSERVATIONS

The observations were carried out using the 85 foot (26 m) telescope of the Hat Creek Radio Observatory (HCRO) in 1987 February and March. The receiver front-end consists of a low-noise HEMT first stage giving a 150 K noise temperature followed by two stages of conventional FET amplification and a post-amplifier. The half-power beamwidth is about 4′, and the single sideband temperature was ∼250 K at 12.2 GHz. The ratio of flux density to antenna temperature is 17 Jy K^{-1}. This ratio implies an aperture efficiency of 30%, which is a low value, about $\frac{2}{3}$ the usual value of ∼50%, and implies that the surface of the telescope is significantly imperfect at this frequency. This is, in fact, consistent with present knowledge of this telescope. The telescope is usable at this frequency, but due care must be taken to obtain accurate measurements by applying pointing corrections and position-dependent gain corrections. The flux density calibration was done by observing Cygnus A, whose flux density at this frequency is 120 Jy. The uncertainty in the flux density scale is about 20%.

For the survey, we fixed the local oscillator so that the line in the terrestrial laboratory would appear at the center of the passband. The 1024 channel correlator was used either with 20 MHz or 10 MHz bandwidth (equivalent to 490 km s^{-1} and 250 km s^{-1}, respectively). The survey covers at least ±50 km s^{-1} with respect to the LSR velocity of the known masers in each source, which should be sufficient because all masers within a given source tend to have similar velocities. The observations were done by integrating only on the source position; the reference spectrum for each source was derived from the spectra of other sources, which was possible because the local oscillator frequency was fixed. The integration time per source ranged from few tens of minutes to 8 hr. Sources detected in this way were observed again in the position switching mode to obtain accurate velocity information. The pointing has not been checked carefully for these sources and the error in flux density due to pointing could be as large as 30%. The nonstellar H_2O maser sources for the survey were taken from the catalog of Dinger and Dickinson (1980); type I OH/IR stars are from Engels (1979). Of the 150 H_2O masers

---

[1] This designation of NGC 6334 follows Rodríguez, Cantó, and Moran (1982) and is used henceforth.

931

observable at HCRO, we excluded the 26 sources observed by Batrla *et al.* (1987) and observed 78 sources, which included all H_2O masers with peak flux densities greater than 50 Jy in the catalog. About half of the sources for the survey have a peak flux density less than 50 Jy. Also, 33 of the 40 observable type I OH/IR stars in Engels' catalog were observed.

The polarization observations were done for five strong masers, including Cepheus A and G188.94+0.89 which we discovered in our survey. The other three sources are W3(OH), NGC 6334F, and NGC 7538, which were detected by Batrla *et al.* (1987). The 1024 channel correlator was used with 0.3125 MHz bandwidth for G188.94+0.89 and NGC 6334F, and with 0.625 MHz for NGC 7538. For W3(OH) and Cepheus A, the correlator was divided into two equal sections with bandwidths of 0.3125 MHz and with 0.15625 MHz, respectively. The spectra were obtained by integrating 6 minutes on source and also 6 minutes off source. The typical rms noise level was about 1 K. A quarter-wave dielectric vane polarizer was installed in the scalar feed in order to measure circular polarization. Each Stokes parameter was determined independently by observing an appropriate pair of orthogonal polarizations; the polarizations were derived by rotating the feedhorn and the polarizer manually.

Determination of accurate Stokes parameters with this manual adjustment of the feedhorn is limited by pointing accuracy, because data at orthogonal polarizations are obtained in completely independent observations taken at different times. For this reason, we paid a great deal of attention to minimizing the effect of pointing errors on observations of orthogonal polarizations. Each pair of orthogonal polarizations was observed as close as possible in time, with the only delay being that required to move the antenna to the service position and manually adjust the feedhorn. This pair of observations was then repeated in reverse order, so as to cancel the effect of pointing errors that change linearly with time. Thus, each pair of orthogonal polarizations was observed with a set of four observations or more. For example, the sequence of events for the two circular polarizations was: observe right-hand circular (RHC); adjust feedhorn; observe left-hand circular (LHC); observe LHC; adjust feedhorn; observe RHC. This procedure was followed for all sources except Cepheus A, for which time

constraints did not allow the repetition of the usual pair of time-reversed measurements. The pointing was usually checked before and after each set of polarization measurement. This could be done very accurately by observing the source at two positions, each displaced by one-quarter beamwidth from the assumed source position in opposite directions. By subtracting two spectra, we could determine the pointing offset very accurately.

We believe that the resulting pointing accuracy was within 15″ in most polarization observations. The error in Stokes parameters Q, U, and V associated with this pointing error is about 2% of the total flux density, I. Unfortunately however, a few sets of observations showed anomalously low total intensities due to some unknown reason. We multiplied these data by appropriate scaling factors: 1.3 for the circular polarization set and one 0°–90° set of NGC 6334F; and 1.2 for the 0°–45° set and 1.4 for the circular set of G188.94+0.89. Final spectra were Hanning-smoothed to yield velocity resolutions of 0.012 km s^{-1} for G188.94+0.89, NGC 6334F, and Cepheus A and of 0.025 km s^{-1} for W3(OH) and NGC 7538. The error (1 σ) in the final Stokes parameters Q, U, and V, including statistical error, is estimated to be less than 3% of the total flux density I.

III. RESULTS AND DISCUSSION

Among 78 nonstellar water masers, 11 new methanol sources were found. These are listed in Table 1 where the galactic coordinates, names, equatorial coordinates, the approximate velocity range of the spectral line features (or the velocity center for a single spectral line), the velocity width (FWHM) of the main Gaussian component, and the peak flux densities are given. Most of the new sources have narrow lines with velocity widths smaller than 1 km s^{-1}, and they are not fully resolved. Four sources, G188.94+0.89, G9.62+0.19, G31.29+0.07, and Cepheus A, are stronger than 100 Jy and are probably masers. The other sources are also thought to be masers because of their narrow lines. Figure 1 shows the spectra of some interesting sources (see also Fig. 2). The profiles in Figure 1 are Hanning-smoothed to yield a velocity resolution of 0.10 km s^{-1} for G9.62+0.19 and G31.29+0.07, and 0.40 km s^{-1} for G8.67−0.36 and W48. The negative results are summarized in

TABLE 1
PARAMETERS OF NEWLY DISCOVERED 12.2 GHz CH$_3$OH SOURCES

Galactic Coordinates	Name	α(1950)	δ(1950)	V_{range} (km s^{-1})	ΔV_{FWHM} (km s^{-1})	Peak Flux Density (Jy)
188.94+0.89.........	...	06^{h}05^{m}53^{s}7	21°39′09″	10–12	0.4	160
0.54−0.85.........	RCW 142	17 47 03.4	−28 53 39	13.7	0.4	6
9.62+0.19.........	...	18 03 16.0	−20 32 01	−5 to 5	0.2	110
8.67−0.36.........	...	18 03 18.6	−21 37 59	40–46	0.6	8
10.47+0.03.........	W31(1)	18 05 40.5	−19 52 23	74.9	0.6	12
12.68−0.18.........	W33B	18 10 58.9	−18 02 39	56.8	0.9	8
21.88+0.02.........	...	18 28 16.1	−09 51 01	19.2	1.1	6
29.95−0.02.........	W43S	18 43 26.7	−02 42 40	96.5	1.0	12
31.29+0.07.........	...	18 45 36.8	−01 29 12	109–113	0.4	140
35.23−1.79.........	W48	18 59 12.8	01 09 13	40–46	0.8	32
109.87+2.11.........	Cepheus A[a]	22 54 27.0	61 45 46	−4.3	0.3	300

NOTE.—The positions are same as those of water masers (Dinger and Dickinson 1980) except for Cepheus A which is determined in this paper. The position error of Cepheus A is order of ±20″ (see text). About half of the line profiles have multiple peaks and only the approximate velocity range of spectral features (or, in case of single line, the velocity center of the line), the velocity width (FWHM) of main Gaussian component, and the peak flux density are given. For G188.94+0.89 and Cepheus A, whose polarization properties are measured, line parameters of all components are given in Table 3.

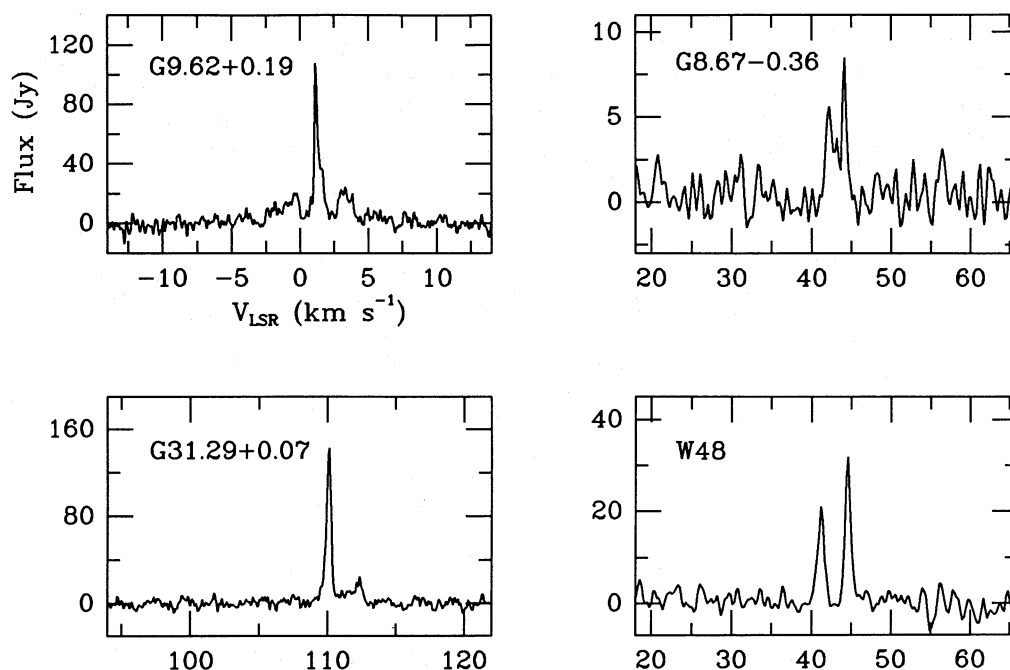[a] This source includes two water masers in our beam.

FIG. 1.—Spectra of 12.2 GHz methanol maser lines detected toward water maser sources. Vertical axis is flux density (Jy), and horizontal axis is LSR velocity (km s^{-1}).

Table 2 where the galactic coordinates, names, equatorial coordinates, and the upper limits to the line are given. The upper limits given in Table 2 are obtained by inspecting individual spectra with eye and correspond to approximately five times the rms sensitivity.

The results of the polarization observations are shown in Figure 2, where the four Stokes parameters I, Q, U, and V are plotted as a function of LSR velocity for each source. We can see that G188.94+0.89, Cepheus A, and NGC 7538 are completely unpolarized, 0% ± 3%, whereas W3(OH) is linearly polarized by ~4% at one velocity. Only NGC 6334F shows a considerable degree of linear polarization. The I spectrum of each source was fitted by several Gaussian components, and their parameters are given in Table 3, where the names, positions, velocity centers, velocity widths (FWHM), and peak total flux densities are given for each component. For W3(OH), we did not try to decompose the spectrum because the line profile is too complex. We did fit each Stokes parameters of NGC 6334F with the same Gaussian components, i.e., with the same velocity center and velocity width. The results are summarized in Table 4 where the velocity center, velocity width, peak total flux density, degree of linear polarization, $[(Q^2 + U^2)^{1/2}/I]$, position angle of ellipse, and degree of circular polarization, (V/I), are given for each component. We can see that each component is linearly polarized up to 10%. Two components appear to have a few percent circular polarization. However, it is probably instrumental because the V spectrum is proportional to the I spectrum, which is the expected result of an error in gain calibration; in any case, it is smaller than our estimated error.

In the survey, we detected methanol masers toward about 15% of water masers. This small fraction may be due to our sensitivity-limited survey. In Figure 3, we plot the peak flux densities of methanol sources, including three strong sources detected by Batrla et al. (1987), as a function of H$_2$O peak flux

densities. The data on water masers are obtained from Genzel and Downes (1977) for W31(1), W33B, W43S, W48, W3(OH), and NGC 7538; from Genzel and Downes (1979) for G9.62+0.19, G8.67−0.36, G21.88+0.02, and G31.29+0.07; from Batchelor et al. (1980) for G188.94+0.89 and RCW 142; from Moran and Rodríguez (1980) for NGC 6334F; and from Rowland and Cohen (1986) for Cepheus A. The dotted horizontal line in Figure 3 is a typical detection limit (~5 Jy) of our survey and the dotted vertical line is 3 times the rms sensitivity of the survey done by Genzel and Downes (1977, 1979).

In Figure 3, we could notice two things: First, no methanol masers were detected toward water masers with flux density less than ~30 Jy even though those sources compose about 30% of our sample. Second, there is a weak trend such that the stronger water masers are also the stronger methanol masers. Since the peak flux density of water masers could change in short time scales, e.g., a few years (Reid and Moran 1981), the relationship should be inspected more carefully by comparing flux densities obtained in the same period of time. However, there is reason to believe that the weaker water masers have "associated" methanol masers with flux density less than our detection limit, so that the real fraction of methanol masers to water masers is larger than 15%. The fraction of methanol masers to water masers increases to 50% (four out of eight) for water masers with flux densities larger than 500 Jy and to 20% (six out of 31) for those with flux densities between 50 and 500 Jy. Also, for the more sensitive Batrla et al. (1987) survey, the fraction is about 40%.

The velocity ranges covered by methanol masers are much narrower than those covered by water masers in general, even excluding high velocity features. This can be seen in Figure 4, which exhibits the methanol velocity versus the H$_2$O velocity. The data on water masers are obtained from the same references as given above. In Figure 4, the filled circles represent the approximate velocity centroids, and the horizontal and vertical

TABLE 2

SUMMARY OF NEGATIVE RESULTS

A. NONSTELLAR H$_2$O MASERS

Galactic Coordinates	Name(s)	α(1950)	δ(1950)	Flux Density Limit (Jy)
117.76 − 3.63	Lk Hα 198	00^{h}08^{m}43^{s}2	58°33′41″	5
123.07 − 6.31	NGC 281, S184	00 49 29.2	56 17 36	7
133.68 + 1.22	W3(1)	02 21 40.8	61 53 26	5
133.75 + 1.20	W3(3)	02 22 06.1	61 50 40	5
138.50 + 1.64	S201	02 59 22.4	60 16 12	7
158.35 − 20.56	HH 7–11 A, B[a]	03 25 57	31 05 32	7
158.39 − 20.57	HH 7–11 C	03 26 05.0	31 03 40	7
176.23 − 20.77	T Tauri	04 19 04.2	19 25 05	8
208.75 − 19.21	OMC 2(2)	05 32 58.0	−05 07 25	7
208.82 − 19.24	OMC 2(1)	05 32 59.9	−05 11 29	7
210.43 − 19.77	HH 1	05 33 52	−06 47 09	3
183.72 − 3.66	GGD 4	05 37 21.8	23 49 24	5
173.72 + 2.70	S235, GGD 5–6	05 37 31.8	35 40 18	5
206.57 − 16.36	NGC 2024, Orion B	05 39 13.7	−01 57 30	7
205.11 − 14.11	NGC 2071	05 44 31.3	00 20 48	7
192.62 − 3.04	MWC 789, HD 250550	05 59 05.5	16 31 10	5
213.70 − 12.61	Mon R2, NGC 2170[a]	06 05 22	−06 22 35	7
189.91 + 0.27	S252A	06 05 35.5	20 30 31	7
189.78 + 0.35	S252A3	06 05 36.6	20 39 44	7
213.88 − 11.82	GGD 12–15	06 08 25.7	−06 10 50	3
214.13 − 11.41	GGD 16–17	06 10 23.0	−06 12 55	3
203.32 + 2.05	NGC 2264	06 38 25.2	09 32 12	7
224.34 − 1.28	GL 1074	07 05 28.5	−10 39 18	3
231.83 + 4.22	OH 0739−14	07 39 58.9	−14 35 38	7
351.16 + 0.70	NGC 6334B	17 16 34.5	−35 54 44	7
5.89 − 0.40	W28A2	17 57 28.7	−24 03 53	7
12.21 − 0.12[a]	...	18 09 45	−18 25 10	3
13.87 + 0.28	...	18 11 41.5	−16 46 34	5
15.03 − 0.67	M17(1, 2, 3)[a]	18 17 30	−16 14 30	7
15.18 − 0.62	M17(4)	18 17 37.0	−16 03 40	9
19.60 − 0.23	...	18 24 50.1	−11 58 22	5
23.95 + 0.15	...	18 31 40.8	−07 57 17	7
24.49 − 0.04	...	18 33 22.8	−07 33 54	7
24.79 + 0.08	...	18 33 30.3	−07 14 42	5
28.86 + 0.07	...	18 41 07.9	−03 38 41	5
31.41 + 0.31	...	18 44 59	−01 16 07	5
30.76 − 0.05	W43Main[a]	18 45 02.8	−02 01 18	7
30.94 + 0.03	W43OH1612	18 45 05.6	−01 48 39	7
30.82 − 0.06	W34Main(3)	18 45 11.0	−01 57 57	7
30.82 − 0.16	W43Main(4)	18 45 33.1	−02 00 21	7
34.25 + 0.16	W44	18 50 46.4	01 11 10	7
40.48 + 2.59	S76W	18 53 34	07 49 45	5
40.50 + 2.54	S76E	18 53 47	07 49 26	5
35.58 − 0.03	...	18 53 51.1	02 16 27	5
40.62 − 0.14	...	19 03 34.9	06 41 55	5
43.16 − 0.03	W49S	19 07 58.2	09 00 03	7
43.80 − 0.12	...	19 09 31.2	09 30 51	5
69.54 − 0.98	ON1, Cygnus 1	20 08 09.8	31 22 42	5
75.77 + 0.34	ON2S, Cygnus 2S	20 19 48.9	37 15 52	5
75.78 + 0.34	ON2N, Cygnus 2N	20 19 51.8	37 17 01	7
76.36 − 0.60	S106, GL2584	20 25 25.0	37 12 30	7
78.89 + 0.71	AFCRL 19, CRL 2591	20 27 36.0	40 01 16	5
81.87 + 0.78	W75N OH	20 36 50.5	42 27 01	5
81.77 + 0.60	W75S(3)[a]	20 37 14	42 14 45	7
105.37 + 9.84	NGC 7129(2), GGD 32–35	21 41 52.0	65 49 40	5
108.20 + 0.59	S146	22 47 31.0	59 39 43	5
80.57 − 44.12	IRC + 10523	22 51 40.0	08 37 54	5
108.66 − 0.86	S152	22 55 38.2	58 33 08	7
111.28 − 0.67	S157	23 13 53.1	59 45 18	7

934

4863..931K

TABLE 2—*Continued*

B. Type I OH/IR Stars

Name(s)	α(1950)	δ(1950)	Flux Density Limit (Jy)
IRC −30033, W Eri	04ʰ09ᵐ26ˢ	−25°15'24"	7
IRC 10060, R Tau	04 25 36	10 03 30	7
IRC 20082	04 26 07	24 37 36	7
IRC 10066, RX Tau	04 35 30	08 13 36	7
IRC 40135, RU Aur	05 35 42	37 36 36	7
AW Tau	05 44 19	27 06 18	9
IRC 60172, U Lyn	06 36 18	59 57 24	5
IRC 10135, FX Mon	06 42 18	09 05 36	9
IRC −20133, Z Pup	07 30 29	−20 32 48	5
231.8 + 4.2	07 39 59	−14 36 12	7
IRC 30195, AU Gem	07 42 16	30 55 54	3
IRC −10222, X Hya	09 33 07	−14 28 00	7
IRC 30215, R LMi	09 42 35	34 44 36	5
IRC 10234, W Leo	10 50 59	13 58 54	5
IRC 20237, R Com	12 01 41	19 03 24	3
IRC 40238, U CVn	12 44 57	38 38 24	7
IRC 10262, RT Vir	13 00 05	05 27 06	3
IRC −30207, W Hya	13 46 13	−28 07 06	7
IRC −30215, RU Hya	14 08 42	−28 38 24	7
IRC 10290, S Ser	15 19 20	14 29 12	7
IRC 30272, S CrB	15 19 21	31 32 48	7
IRC 20298, U Her	16 23 35	19 00 18	7
IRC 10314, RX Oph	16 50 22	05 28 54	5
CRL 1937, RW Sco	17 11 36	−33 22 36	7
IRC 10342, RT Oph	17 54 11	11 10 30	7
IRC −20424	18 00 58	−20 19 30	7
IRC −10414	18 20 28	−13 44 06	7
IRC 30360, V Lyr	19 07 07	29 34 42	15
IRC 10433, RT Aql	19 35 36	11 36 18	15
IRC −10524, GY Aql	19 47 20	−07 44 18	19
IRC −30419, RR Sgr	19 52 50	−29 19 24	19
IRC 10498, UU Peg	21 28 38	10 56 18	7
IRC 30481, TW Peg	22 01 41	28 06 30	7

Note.—The positions as given by Dinger and Dickinson 1980 and Engels 1979 are used for nonstellar water masers and for stellar masers, respectively.

[a] These sources include two or three water masers in our beam, and their mean positions are given.

TABLE 3

Parameters of Five Strong CH₃OH Masers

Name	α(1950)	δ(1950)	V_{LSR} (km s⁻¹)	ΔV_{FWHM} (km s⁻¹)	Peak Total Flux Density (Jy)
W3(OH)[a]	02ʰ23ᵐ17ˢ0	61°38'53"	−44.86	...	900
G188.94 + 0.89	06 05 53.7	21 39 09	10.41(0.02)	0.37(0.02)	155 (6)
			10.83(0.02)	0.37(0.08)	112 (6)
			11.18(0.02)	0.31(0.03)	114 (12)
NGC 6334F[a]	17 17 32.3	−35 44 04	−11.39(0.01)	0.36(0.01)	1010 (10)
			−11.03(0.01)	0.20(0.01)	331 (17)
			−10.61(0.01)	0.37(0.01)	886 (28)
			−10.19(0.14)	1.14(0.20)	103 (9)
Cepheus A	22 54 27.0	61 45 46	−4.27(0.01)	0.29(0.01)	302 (7)
NGC 7538[a]	23 11 36.5	61 11 47	−61.41(0.02)	0.21(0.07)	19 (5)
			−61.04(0.08)	0.82(0.15)	17 (2)
			−56.48(0.01)	0.82(0.01)	230 (2)

Note.—For sources with multiple peaks, the line parameters of each Gaussian component are given. For W3(OH), however, we did not try to decompose the spectrum because the profile is too complex (see Fig. 2). The velocity quoted is the value at peak flux density. Errors quoted are 3 σ deviations from Gaussian fits.

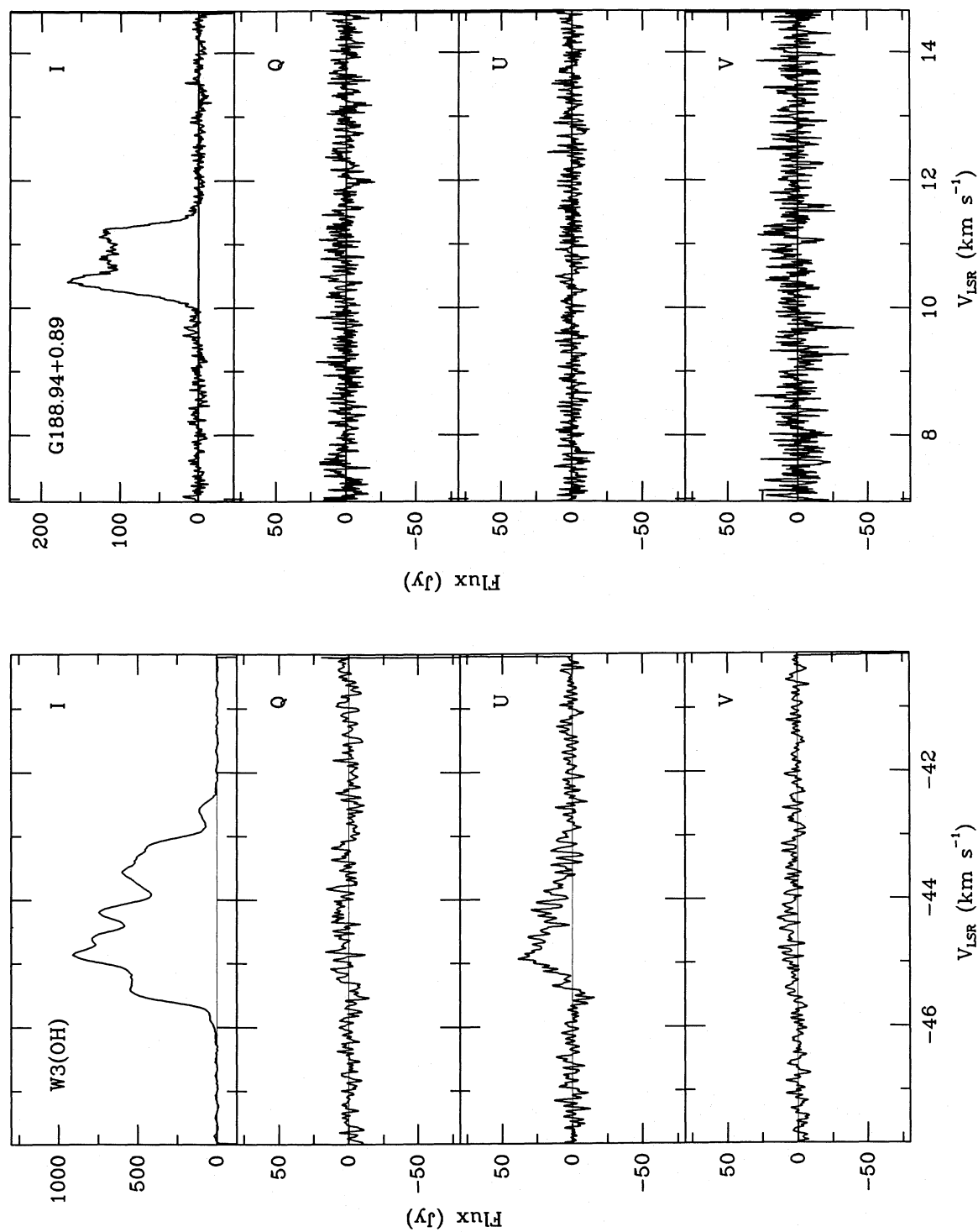[a] The positions of these sources are obtained from Batrla *et al.* 1987.

935

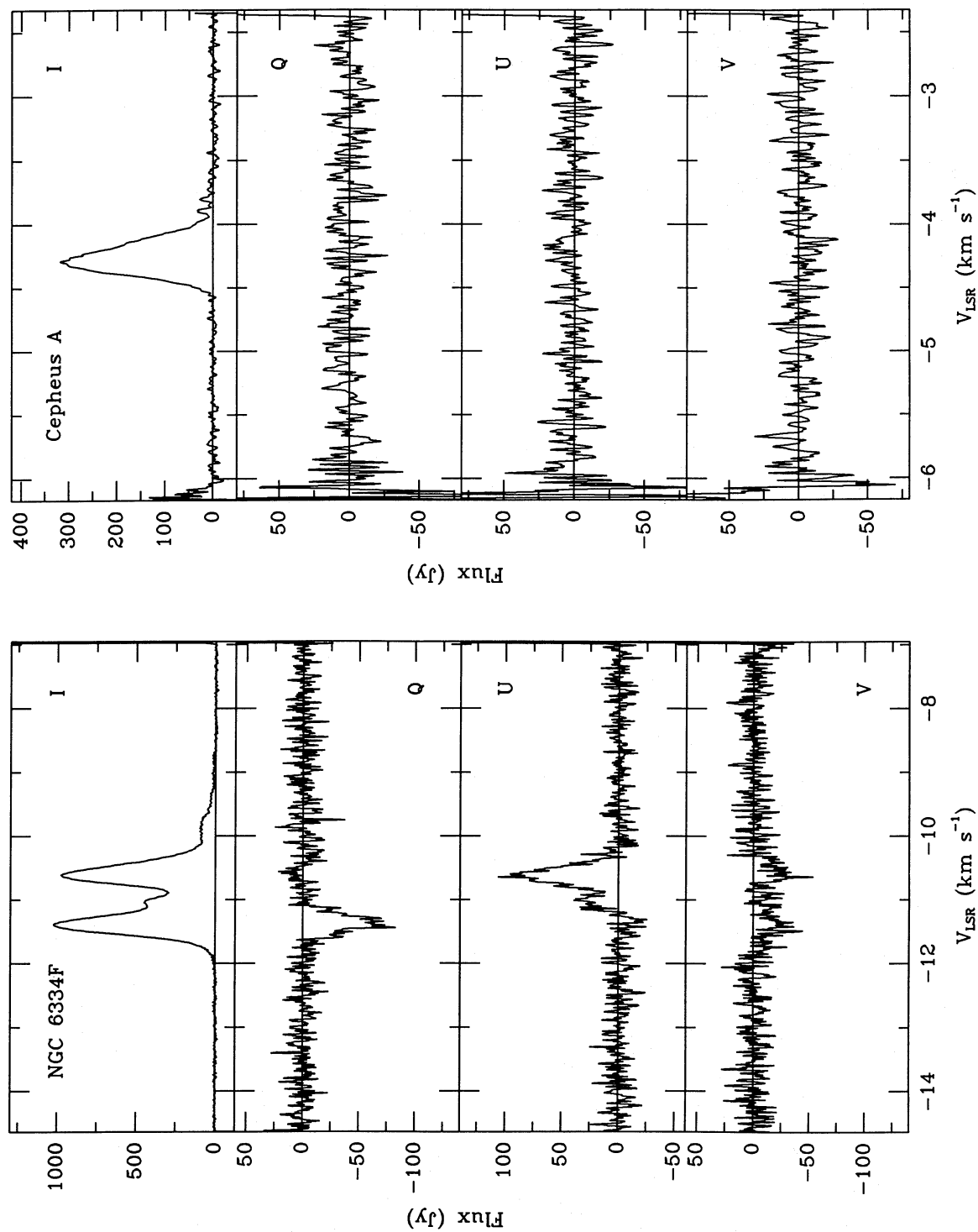FIG. 2.—Stokes parameters for five strong methanol masers
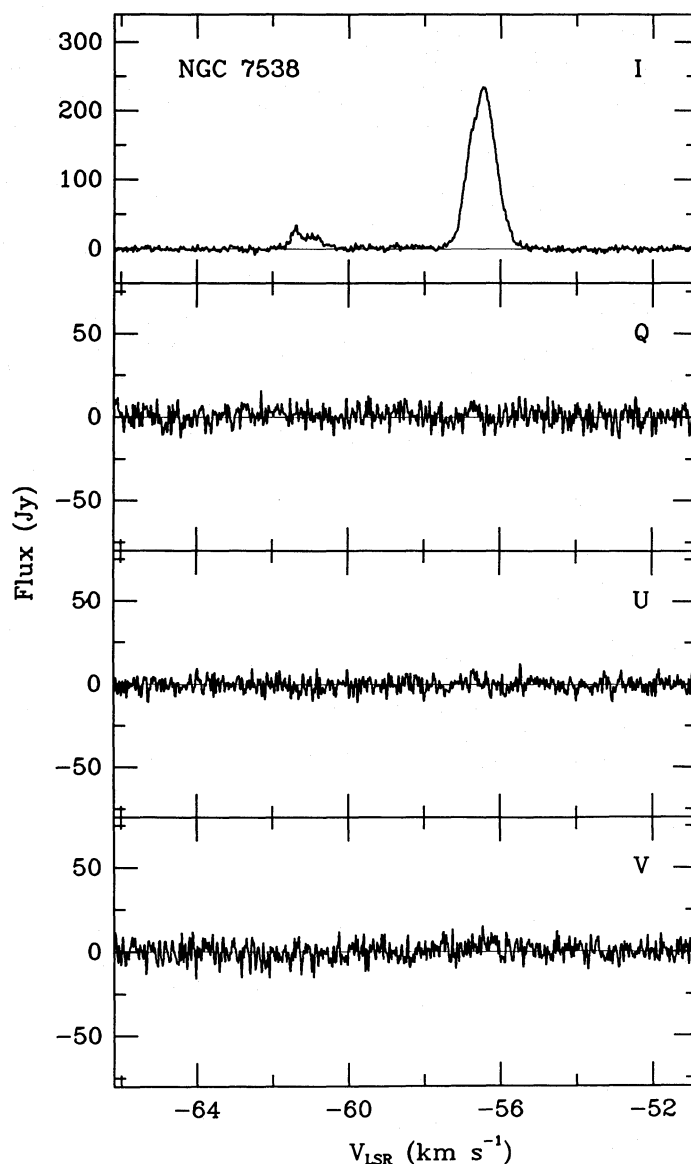
FIG. 2.—Continued

FIG. 2.—*Continued*

lines represent the velocity ranges of water masers and methanol sources, respectively. For the case of methanol masers, the velocity ranges are all smaller than 10 km s^{-1}, whereas for H_2O masers they are generally bigger than 10 km s^{-1} (excluding single lines). Also, the velocity range of a methanol maser does not overlap exactly with that of the associated water masers in many cases. This suggests that the methanol masers occur in spatially different regions from water masers, and also that they are not composed of as many components as water masers are. However, since the difference in the overlap of velocity range is usually small and since there is a weak relation between their intensities as we noted above, we cannot disregard the physical association between methanol masers and water masers. Batrla *et al.* (1987) noted that the velocity range of their three strong methanol sources overlap with OH velocity ranges and also that, in the case of W3(OH), the

TABLE 4

POLARIZATION PROPERTIES OF NGC 6334F

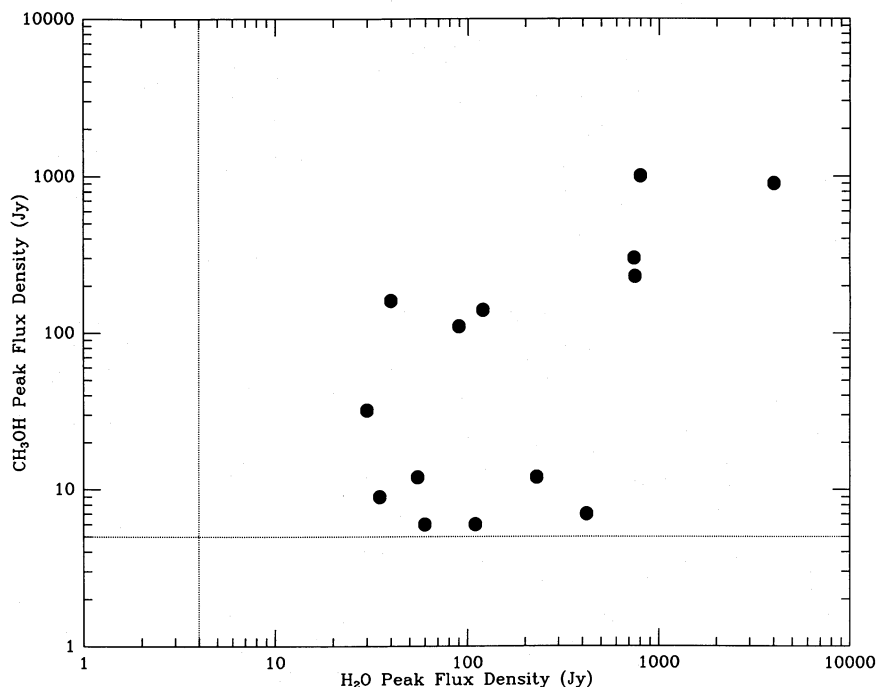| Component	V_{LSR} (km s^{-1})	ΔV_{FWHM} (km s^{-1})	Peak Total Flux Density (Jy)	Degree of Linear Polarization	Position Angle	Degree of Circular Polarization[a]
1...............	−11.39	0.36	1010	6%	90°	2%
2...............	−11.03	0.20	331	9	45	...
3...............	−10.61	0.37	886	10	45	3

[a] See text.

FIG. 3.—Peak flux density (Jy) of methanol masers plotted against peak flux density of water masers. Dotted horizontal line represents our detection limit. Dotted vertical line represents 3 times rms sensitivity of water maser survey done by Genzel and Downes (1977, 1979).

$2_0 \rightarrow 3_{-1}$ emission covers exactly the same velocity interval as the other methanol lines, which have been shown to be coincident with the position of OH masers (Menten *et al.* 1985).

No decisive information is available on the spatial relationship of the $2_0 \rightarrow 3_{-1}$ *E* methanol masers with H_2O or OH masers. For NGC 6334F and NGC 7538, Batrla *et al.* (1987) performed several offset measurements and stated that the methanol masers are coincident with compact H II regions

within their pointing errors, $\pm 15''$. However, in NGC 6334F the OH maser is $20'' \pm 1''$ south of the compact H II region, while the H_2O maser is $\sim 30'' \pm 30''$ south of the compact H II region (Moran and Rodríguez 1980; Rodríguez, Cantó, and Moran 1982). Thus, according to the results of Batrla *et al.*, the methanol maser in NGC 6334F is offset from the OH maser by $20'' \pm 15''$ and also possibly from the H_2O maser.

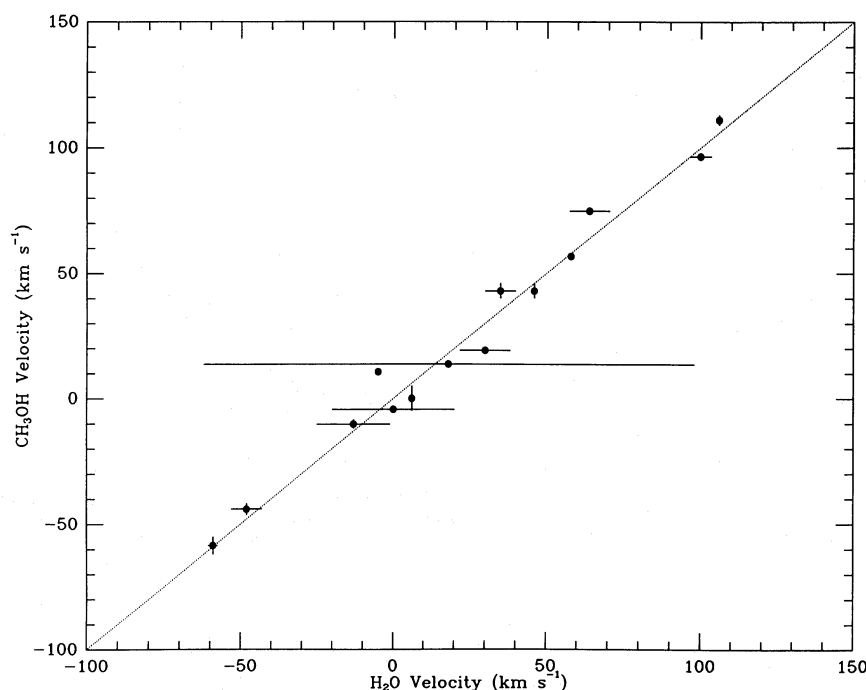In NGC 7538, the H_2O and OH masers lie in two groups

FIG. 4.—Radial velocity of methanol masers plotted against radial velocity of water masers. Filled circles represent approximate velocity centroids. The radial velocity ranges of the methanol and water masers are indicated by the vertical and horizontal lines, respectively.

separated by 80″ (e.g., Forster *et al.* 1978). One group is associated with IRS 1, with velocities of -61 km s^{-1} and ~ -59 km s^{-1} for the H_2O and OH masers, respectively (e.g., Forster *et al.* 1978; Norris *et al.* 1982). These velocities are rather close to the velocity of the weak methanol feature, ~ -61.2 km s^{-1}. The close coincidence in both position and velocity suggests that all three types of maser are associated. However, the velocity of the strong methanol maser feature is -56.5 km s^{-1}, which is very different from those of the IRS 1–associated masers. Therefore, the strong methanol feature must arise from a different region. It is interesting to note that the velocity of the strong methanol feature is close to those of the masers in the second H_2O/OH maser group located about 80″ south from IRS 1; however, the 80″ displacement again rules out a true physical association.

We measured the methanol maser position for Cepheus A. The position could be determined accurately with respect to that of NGC 7538 because they are only about 2° apart in the sky. We believe that our relative positional accuracy is $\pm 20″$, but cannot be absolutely certain because we only made the measurement once. If our measurement is correct and if Batrla *et al.* are correct in stating that the strong methanol maser feature in NGC 7538 has the same position as IRS 1, then the methanol maser in Cepheus A lies 60″ $\pm$ 20″ east of the OH and H_2O masers (e.g., Lada *et al.* 1981). At a distance of 700 pc (Blaauw, Hiltner, and Johnston 1959), the methanol maser is then about 0.2 pc from the compact H II region. Even though it is not very unusual to observe masers far away from the known power sources, e.g., the OH maser in NGC 6334F (0.16 pc; Rodríguez, Cantó, and Moran 1982) and the $6_2 \rightarrow 6_1$ methanol masers in W33, W51, and DR 21 (0.9 pc, 3.4 pc, and 1.1 pc, respectively; Menten *et al.* 1986), such widely separated masers require other power sources.

In summary, there are indications that the $2_0 \rightarrow 3_{-1}$ *E* methanol masers emerge from regions apart from other H_2O and OH masers. However, positional uncertainties with single-dish measurements are too large to make absolutely definitive statements, and interferometric observations of methanol masers are needed.

The absence of circular polarization in most methanol masers can be understood in the same context as for water masers (Bologna *et al.* 1975). A necessary condition for circular polarization (Goldreich, Keeley, and Kwan 1973) is that the Zeeman splitting be greater than the line width (2×10^4 Hz). Since the Lande *g*-factor is small for the ground electronic state of methanol, $\sim 10^{-4}$ (Townes and Schawlow 1955), the magnetic field strength required for this condition is ~ 70 G. The magnetic field strength in water maser regions is probably not bigger than 1 G (Reid and Moran 1981); thus, no circular polarization is expected for the associated methanol masers. The detection of two linearly polarized methanol sources out of five is a similar probability to that obtained from Bologna *et al.* (1975) and Knowles and Batchelor (1978) on water masers. They found that about 25% of water masers show linear polarization ranging from few percent to 50%, but mostly less than 20%. According to Goldreich, Keeley, and Kwan (1973), the partial linear polarization is possible for saturated masers with sizeable magnetic field strength. The limit on the magnetic field strength depends on the source geometry, which is not known but expected to be similar to the strength in water maser sources.

REFERENCES

Barrett, A. H., Schwartz, P. R., and Waters, J. W. 1971, *Ap. J (Letters)*, **168**, L101.
Batchelor, R. A., Caswell, J. L., Goss, W. M., Haynes, R. F., Knowles, S. H., and Wellington, K. J. 1980, *Australian J. Phys.*, **33**, 139.
Batrla, W., Matthews, H. E., Menten, K. M., and Walmsley, C. M. 1987, *Nature*, **326**, 49.
Blaauw, A., Hiltner, W. A., and Johnston, H. L. 1959, *Ap. J.*, **130**, 69.
Bologna, J. M., Johnston, K. J., Knowles, S. H., Mango, S. A., and Sloanaker, R. M. 1975, *Ap. J.*, **199**, 86.
Buxton, R. B., Barrett, A. H., Ho, P. T. P., and Schneps, M. H. 1977, *A.J.*, **82**, 985.
Dinger, A., and Dickinson, D. F. 1980, *A.J.*, **85**, 1247.
Engels, D. 1979, *Astr. Ap. Suppl.*, **36**, 337.
Forster, J. R., Welch, W. J., Wright, M. C. H., and Baudry, A. 1978, *Ap. J.*, **221**, 137.
Genzel, R., and Downes, D. 1977, *Astr. Ap. Suppl.*, **30**, 145.
———. 1979, *Astr. Ap.*, **72**, 234.
Goldreich, P., Keeley, D. A., and Kwan, J. Y. 1973, *Ap. J.*, **179**, 111.
Hills, R., Pankonin, V., and Landecker, T. L. 1975, *Astr. Ap.*, **39**, 149.

Knowles, S. H., and Batchelor, R. A. 1978, *M.N.R.A.S.*, **184**, 107.
Lada, C. J., Blitz, L., Reid, M. J., and Moran, J. M. 1981, *Ap. J.*, **243**, 769.
Menten, K. M., Johnston, K. J., Wilson, T. L., Walmsley, C. M., Mauersberger, R., and Henkel, C. 1985, *Ap. J. (Letters)*, **293**, L83.
Menten, K. M., Walmsley, C. M., Henkel, C., and Wilson, T. L. 1986, *Astr. Ap.*, **157**, 318.
Moran, J. M., and Rodríguez, L. F. 1980, *Ap. J. (Letters)*, **236**, L159.
Morimoto, M., Ohishi, M., and Kanzawa, T. 1985, *Ap. J. (Letters)*, **288**, L11.
Norris, R. P., Booth, R. S., Diamond, P. J., and Porter, N. D. 1982, *M.N.R.A.S.*, **201**, 191.
Reid, M. J., and Moran, J. M. 1981, *Ann. Rev. Astr. Ap.*, **19**, 231.
Rodríguez, L. F., Cantó, J., and Moran, J. M. 1982, *Ap. J.*, **255**, 103.
Rowland, P. R., and Cohen, R. J. 1986, *M.N.R.A.S.*, **220**, 233.
Townes, C. H., and Schawlow, A. L. 1955, *Microwave Spectroscopy* (New York: McGraw-Hill).
Wilson, T. L., Walmsley, C. M., Menten, K. M., and Hermsen, W. 1985, *Astr. Ap.*, **147**, L19.
Wilson, T. L., Walmsley, C. M., Snyder, L. E., and Jewell, P. R. 1984, *Astr. Ap.*, **134**, L7.

DONALD C. BACKER, CARL HEILES, BON-CHUL KOO, and DAVID R. W. WILLIAMS: Astronomy Department, University of California, Berkeley, CA 94720